Performance assessment of a mathematical morphology ship detection algorithm for SAR images through comparison with AIS data.

R. Grasso[1], S. Mirra[2], A. Baldacci[3], J. Horstmann[1], M. Coffin[1], M. Jarvis[4]
[1]*NATO Undersea Research Centre (NURC), Viale San Bartolomeo, 400, 19126, La Spezia, Italy, {grasso, horstmann, coffin}@nurc.nato.int*
[2]*Italian Navy*
[3]*NSIGHT SAS, Italy*
[4]*SPAWAR System Center, Pacific, mel@spawar.navy.mil*

Abstract

This paper describes a procedure to evaluate the performance of ship detection algorithms for Synthetic Aperture Radar (SAR) using real SAR images and Automatic Identification System (AIS) data as ground truth. Accurate AIS-SAR data association is achieved by correcting the AIS data for the SAR induced position errors by exploiting SAR acquisition parameters and vessel state information (speed and course) provided by AIS tracks. The methodology has been tested on a ship detection algorithm based on mathematical morphology which is described in this paper. The evaluation has been carried out on a RADARSAT-2 data set including images at different acquisition modes which was collected in the Mediterranean Sea. Estimates for the detection and the false alarm probability, and the contact position error are provided.

1. Introduction

This paper describes a methodology to automatically assess the performance of ship detectors for Synthetic Aperture Radar (SAR) by means of real data. In particular, detector contacts from a set of real SAR images are compared with Automatic Identification System (AIS) contacts. Estimates of the detection (P_d) and the false alarm probability (P_{fa}), and the contact position error (ε_p) are provided. The procedure is useful to validate detector performance, to make comparisons among different processing schemes and sensors, and to initialize the input parameters of data association and tracking algorithms which fuses information from different sources to provide an integrated maritime surveillance picture of an area of interest [1], [2].

The performance assessment of a ship detection algorithm developed at NURC, which is based on mathematical morphology [3], is provided. The SAR data set used to evaluate the detector consists in a series of 60 RADARSAT-2 images collected using different acquisition modes over the Mediterranean Sea. In order to avoid building a ground truth data set by visual inspection of the whole set of SAR images, AIS contacts are used as ground truth. A nearest neighbor association procedure is used to associate an AIS contact to a SAR contact. Associated SAR contacts are considered as detected target, while not-associated contacts are declared as false alarms.

Particular care has been taken to correct contacts position errors induced by SAR related Doppler effects [4]. The relative AIS-SAR position shift is automatically corrected before comparing AIS and SAR contacts in order to reduce association errors and improve the performance estimate.

The analysis provides an average position error ε_p of 175 m with a P_d of 80% and a P_{fa} bound of 7e-5%. The performance analysis has been carried out also on single clusters of images acquired with the same acquisition mode. Results are provided for each cluster so as to compare the acquisition modes.

The paper is organized as follows. Section 2 provides a general introduction to the performance assessment methodology including position error corrections. Section 3 describes the mathematical morphology ship detection algorithm. Section 4 describes the data sets used for performance estimation. Section 5 reports the results of the investigation. The paper ends with the conclusions and future work.

2. Performance estimation

Figure 1 shows the schematic of the proposed procedure. The procedure accepts as inputs the AIS data set acquired over the area of interest in a time frame that include the SAR image acquisition time, the SAR acquisition parameters and the data set of SAR contacts at the detector output. The output is an estimate of ε_p, P_d and an upper bound for P_{fa}.

The following subsections detail the key processing steps of the procedure *i.e.* the AIS contact selection,

978-0-7695-3872-3/09 $26.00 © 2009 IEEE
DOI 10.1109/ISDA.2009.99

correction of AIS position for SAR induced position errors, automatic AIS-SAR contact association and estimation of performance parameters.

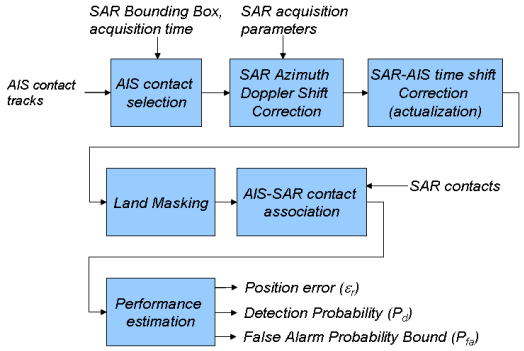

Figure 1. Schematic of the performance procedure estimation.

2.1. AIS data and contact selection

AIS is a system used for cooperative tracking, identification of vessels and for navigation safety and security, and is widely employed in maritime surveillance. It is based on transponders installed on the ship (operating in the VHF spectrum) that broadcast messages of vessel information like the vessel's Maritime Mobile Service Identity (MMSI), which is a unique nine digit identification number, the position, the course over ground (COG), the speed over ground (SOG), and the vessel name. The messages are transmitted every 2-10 seconds depending on the vessel speed, and every 3 minutes when vessel is at anchor. The vessel state is generated from the ship's navigational sensors, typically the global navigation satellite system (GNSS) receiver and the gyrocompass. The signals are received by AIS transponders installed on other ships or on land based systems.

The fusion of AIS data with data from non-cooperative sensors like radars is an emerging and promising way to improve surveillance capabilities. Information from these sources provides contact confirmation, coverage in areas not reached by AIS receivers and information for those vessels not having AIS transponders installed on board. On the other hand, due to random disturbances generated by sea clutter and apparatus internal noise, non-cooperative sensors are only able to detect targets with a non-zero probability of false alarm and a probability of detection less than one.

The analysis of the detection performance of non-cooperative sensors is important for the fusion and tracking blocks of the surveillance system in order to initialize the data association and filtering procedures. The use of trial data allows the performance to be estimated for a real operational scenario involving different sea clutter conditions and SAR acquisition modes. AIS contacts are used as ground truth and allow the procedure to run automatically without the need for a human operator to inspect the SAR image to build the ground truth data set.

AIS messages are massive and a pre-selection of data useful for the analysis has to be carried out before any other step. The database of AIS messages available at NURC is searched using the MMSI number as key to arrange tracks of vessels within the bounding box of the SAR image, in a temporal interval centred on the image acquisition time. The information provided by the vessel tracks (position, SOG and COG) together with sensor geometry configuration, is used in the next step to correct the position of AIS contacts and compensate for SAR position errors. This allows the procedure to achieve a high degree of confidence in data association.

2.2. Correction of AIS contact position

Position error along the SAR azimuth direction is observed for those targets having a high range velocity component [4]. The target speed is not known by the SAR processor so that it is not able to correct the Doppler shift in the signal backscattered by the target.

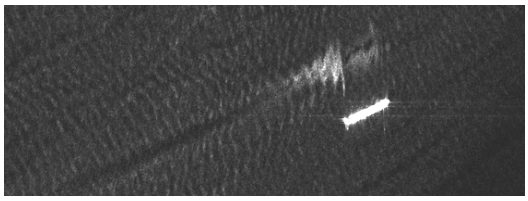

Figure 2. Effects of SAR azimuth shift on a vessel target.

The effect of this phenomenon is observable in the SAR image as depicted in figure 2, where it is possible to see the vessel image that is not aligned with its wake. Knowing the SAR viewing geometry and the target velocity and direction (see figure 3 for the reference system), the azimuth shift of the target, ΔY, can be estimated using the following relationship:

$$\Delta Y = \frac{H \tan(\theta) v \cos(\phi)}{V_s}, \qquad (1)$$

where H is the satellite height, θ the SAR incidence angle, v the target speed magnitude, ϕ the vessel course with respect to the SAR range direction and V_s is the SAR platform velocity.

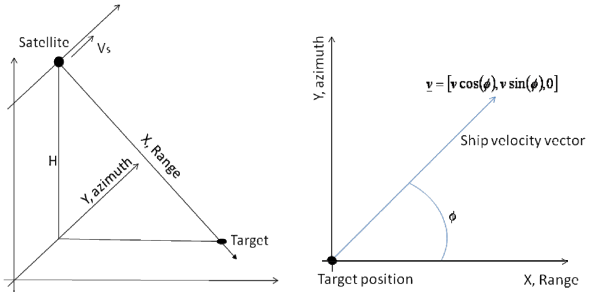

Figure 3. Geometry for SAR azimuth shift computation [4].

The azimuth shift must be taken into account when trying to estimate the detector performance. If the position error is not adequately compensated, association errors between SAR and AIS contacts may occur more frequently, providing wrong estimation of the detector performance. The strategy followed to reduce the estimation error is based on the knowledge of the vessel SOG and COG provided by AIS tracks. This information is integrated with satellite and SAR viewing geometry parameters (satellite height and speed, and SAR incidence angle) to estimate the azimuth shift through (1). The AIS contact acquired at the closest time to the SAR acquisition time is selected from the vessel AIS tracks within the area of interest. The azimuth shift is calculated supposing that the SOG and the COG do not change within the time interval between the SAR image and AIS contact acquisition times. The AIS contact position is compensated for the estimated azimuth shift.

Figure 4 shows an example of AIS position error correction. The considered AIS ship track is mainly oriented along the SAR cross track direction so that the azimuth shift is close to the maximum according to (1). The estimated error is of the order of 960 m. Once compensated along the SAR track direction, the AIS contact is aligned to the SAR contact along the vessel track. The residual error after azimuth position error correction is mainly due to the time shift between the AIS contact and the SAR image acquisition instants. The error is compensated by using the SOG and the COG provided by the AIS contact message. In order to calculate the time shift between the AIS contact and the SAR image, the SAR reference time is taken in the middle of the image acquisition interval, ΔT_{SAR}. In this way, the maximum absolute error in the time shift estimate is $\Delta T_{SAR}/2$. In figure 4, the error for the considered AIS track is 935 m. Once compensated, the AIS contact position error with respect to the SAR contact position is 173 m that is reduced by a factor of 10 with respect to the original error.

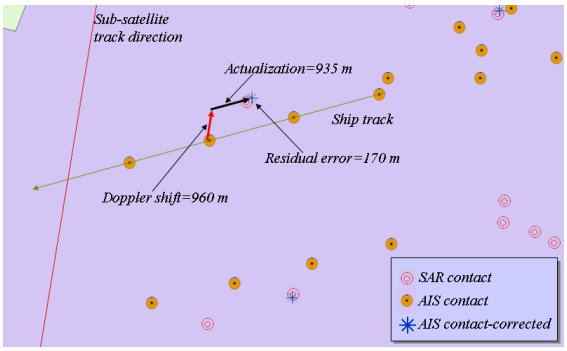

Figure 4. Example of AIS contact positional error correction.

2.3. AIS-SAR contact association

The AIS-SAR contact association is then carried out automatically using a nearest neighbour procedure. The SAR contact having the minimum distance from the AIS contact is selected and if the distance is less than a predefined threshold then the two contacts are associated. The SAR contacts not associated to any AIS contact are considered as false alarms. This is in principle not true due to the possible presence of ships not installing the AIS transponder. The performance measure for false alarm is then a bound which can be used for comparing different detectors on the same set of data. The bound provides a conservative performance measure *i.e.* the actual false alarm rate may be better than the estimated bound.

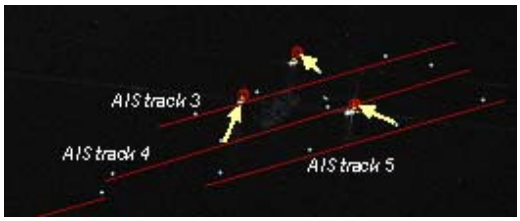

Figure 5. Example of AIS position correction and association with SAR contact.

Figure 5 provides an example of AIS-SAR contact association. Arrows display the spatial correction applied to the AIS contact before SAR contact association procedure. The picture is an example of possible wrong contact association if the positional error is not adequately compensated. Red circled symbols represent the AIS contact corrected for SAR position error and associated to the SAR contact. The arrows display the applied total correction. A nearest neighbor association without previous error position

correction would have been resulted in an association error for contacts belonging to track 3, 4 and 5.

2.4. Performance estimation

Detector performance measurements are provided for a predefined set of detector parameters. The performance indices are the detection probability rate, the bound for false alarm rate and the statistics for positional error.
The probability of detection is simply estimated by the ratio between the number of associated SAR contacts to the total number of AIS contacts. The SAR contacts not associated to an AIS contact are then used to estimate the bound for the false alarm rate by comparing that number to the total number of image pixels on the sea in which no ships were detected. The statistics of the positional error are evaluated on the whole set of associated SAR contacts. The AIS contacts are taken as reference and the position error is the distance between the AIS contact and the associated SAR contact. The statistics provided are the mean and the variance of the distance and the 99% Circular Error Probable (CEP). Positional error indices are compared with the same obtained without correcting for SAR induced position error and acquisition time shift to assess the effectiveness of the correction procedure. The set of performance indexes are evaluated on the aggregated data set of SAR contacts as well as for each single class of SAR acquisition mode. To this purpose, the SAR image data set is segmented so as to have homogeneous clusters of images collected with the same acquisition parameters (resolution, swath width, mean incidence angle and polarization).

3. Detection Algorithm

This section describes the ship detection algorithm considered in this study. Figure 6 shows the building blocks of the system. A comprehensive introduction to mathematical morphology tools is provided in [3] while a detailed description of the morphological detection algorithm can be found in [5]. An introduction to the state of the art of ship detection algorithms for SAR data is provided in [6].
The core of the processing chain is the morphological filtering block that is used to estimate the sea clutter local level adaptively in space and to provide a detection threshold to assure the constant false alarm rate (CFAR) property of the detector.

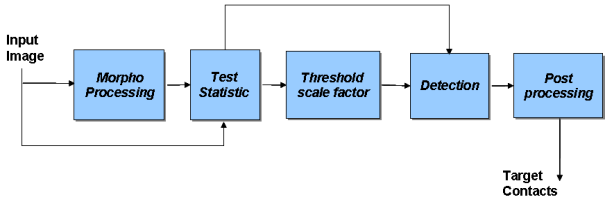

Figure 6. Basic schematic of the ship detection algorithm for SAR images.

The input image amplitude and the output from the filtering block are then combined to build the statistic used to detect ships through a simple threshold test. After detection, the retrieved contacts are then post processed in order to further reduce false alarms.

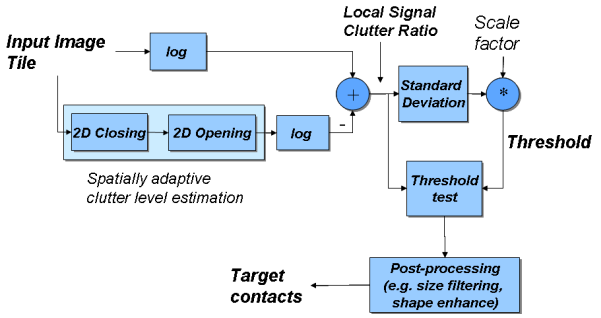

Figure 7. Detector morphological processing block schematic.

Figure 7 details the filtering step and the test statistic calculation. The estimation of the clutter level is achieved by a cascade of two dimensional morphological filters: closing and opening. An example of the output of the cascade of these operations is given in figure 8.

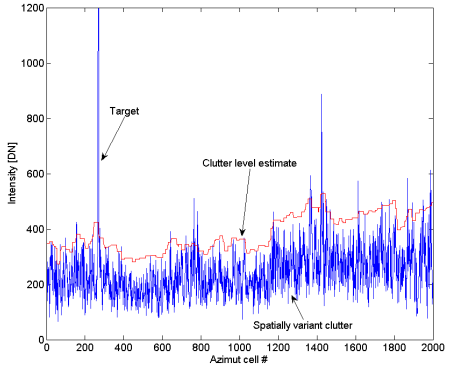

Figure 8. One dimensional example of the signal at the output of the morphological filtering step.

The test statistic consists in the local signal to clutter ratio (SCR) calculated logarithmically. Under the null hypothesis (target not present) the SCR is spatially homogeneous so that a constant threshold can be applied to the SCR to detect targets. The threshold is

calculated making the hypothesis that the target size is significantly less than the size of the processed image tile. Under this hypothesis, the standard deviation of the clutter statistic can be evaluated by the standard deviation of the statistic over the whole processed scene. The final threshold is then obtained multiplying the standard deviation by a constant factor in order to control the level of false alarms.

4. Data set description

The data set used to evaluate the detector consists in 60 RADARSAT-2 images with AIS data associated picked out from a larger data set of 120 images acquired in four key areas for Mediterranean Sea ship traffic, which are the Strait of Gibraltar, the Strait of Sicily, the Ionian Sea and the Bosporus. The data set covers three weeks of acquisitions from 15 October to 8 November 2008.

Table 1. SAR image acquisition modes for the RADARSAT-2 data set.

	Cluster 1	Cluster 2	Cluster 3	Cluster 4
Beam Mode	EH 1-6	S7	SCN A-B	SCW A
Pixel Size [m]	12.5	12.5	25	50
Acquisition Type	High Incidence	Standard	Scan SAR Narrow	Scan SAR Wide
Polarizations	HH	HH HV	HH HV	HH HV

Table 1 shows the features of the four clusters in which the 60 images were segmented on the base of the acquisition beam mode. The clusters are characterized by different combinations of pixel spacing value, polarization, swath width and incidence angle.

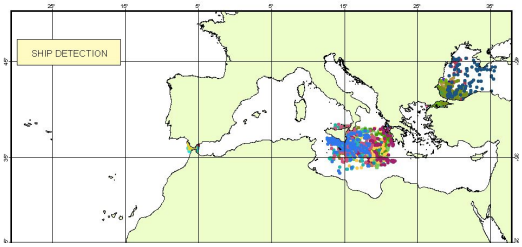

Figure 9. SAR contacts area coverage.

The images were processed by the morphological detector using a squared window filtering size of 13 pixels and a threshold scale factor of 3.3. By varying one of the parameters, such as the scale factor, a Receiver Operating Characteristic (ROC) curve can be retrieved. Moreover, by clustering ship contacts with respect to the SCR, a full range of parametric ROC curves can be constructed each curve representing the receiver performance for a specific class of target. This will be addressed in future work. The whole data set of contacts at the output of the detector is reported in figure 9 showing the four areas covered by the SAR image data set.

5. Results

The performance estimation procedure is applied to the data set of potential ship contacts retrieved as described in the previous section. The results on the aggregated set of contacts and for each class of image are reported.

5.1 Aggregated contact average performance

The position error before and after the AIS contact correction for SAR azimuth displacement and SAR-AIS temporal shift is first evaluated. Figure 10 shows the average position error when the error correction is applied and without correction.

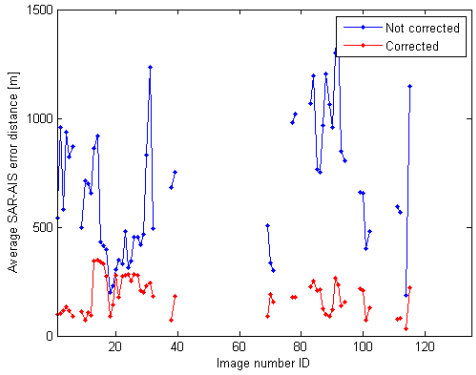

Figure 10. Average AIS-SAR contact distance.

Table 2 summarizes the error position statistics. The mean error averaged on the whole set of images is 707 m before the correction and reaches 175 m after the correction that means an improvement factor of roughly 4. The 99% CEP is improved by the same factor while the standard deviation goes from 790 to 92 meter.

Figure 11 shows the scatter plot of P_d versus the P_{fa} bound for the whole dataset. The image clusters are highlighted by different colors to provide their relative position and dispersion degree. The detection performance is quite variable depending on the specific acquisition mode of a single image. The estimates are calculated for the contacts after position error correction. The average P_{fa} bound achieved is 7e-005% while the P_d is 82 %.

Table 2. Aggregated position error statistics.

	CEP 99% [m]	ε_p [m]	ε_p St Dev [m]
Not corrected	1713	707	790
Corrected	425	175	92

5.2 Segmented data set results

This section reports the results achieved by single image cluster. Table 3 summarizes the average detection and position performance for each image type.

Table 3. Average performance measures for each image cluster.

	Cluster 1	Cluster 2	Cluster 3	Cluster 4
Pfa Bound %	13.7e-5	1.9 e-4	2.7 e-5	8 e-6
Pd %	92	57	45	70
CEP 99% [m]	325	1590	525	470
ε_p [m]	138	656	218	194
ε_p St Dev [m]	72	6	113	102

Cluster 1 has the best performance in terms of P_d=92% and location error that is 138 m in average, with a P_{fa} of 13.7e-5%. The other classes have a P_{fa} bound between 8e-6% and 1.9e-4%, lower P_d between 0.45 and 0.70 and higher location error (between 194, 565 m). The mean performance on the whole data set is P_d=82%, P_{fa}=7e-5% and average position error of 175 m. Better performance in cluster 3 and 4 may be achieved adapting the filtering window size with respect to the pixel size.

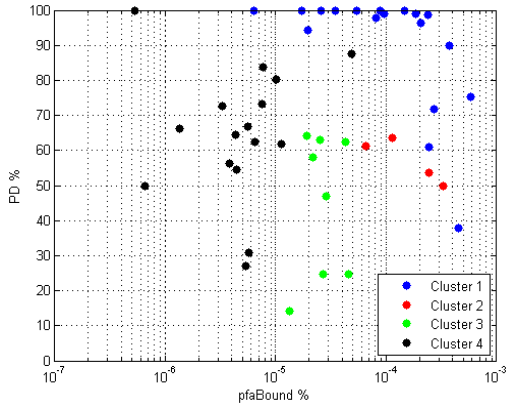

Figure 11. Scatter plot of P_d versus P_{fa} after position correction with SAR data set clustering.

6. Conclusion

This paper describes a procedure for estimating the performance of ship detection algorithms which makes use of SAR data and AIS contact data as ground truth, providing estimates for the P_d, P_{fa} bound and SAR-AIS relative position error statistics. The procedure has been tested on a SAR ship detection algorithm based on mathematical morphology developed at NURC.

The evaluation has been carried out on RADARSAT-2 images collected with different acquisition modes in the Mediterranean Sea.

The performance evaluation has been carried out on the aggregated data set and on single clusters of images having same acquisition parameters. The performance achieved by the detector on the overall data set is P_d=82%, P_{fa}=7e-5% and average position error equal to 175 m with a standard deviation of 92 m. Cluster 1 achieved the best performance among the other clusters with P_d=92%, P_{fa} of 13.7e-5% and average location error of 138 m. The study demonstrated that the procedure for azimuth correction is effective in reducing the relative position error between AIS and SAR contacts even if a mean SAR incidence angle is used in equation (1).

Future work includes estimation of a full mean ROC curve by varying the threshold scale factor of the ship detection algorithm and comparison with other commercially available ship detection algorithms. The extension to other SAR sensor will be also considered.

7. References

[1] Blackman S., Popoli R., "Modern Tracking Systems", Arthech House, Boston-London.

[2] Stove Andrew G., Hurd David L., "Performance Evaluation For Modern Radars", proceedings of 2003 IEEE Radar Conference, Adelaide Australia, 3-5 September 2003 pp. 547-553.

[3] Soille, P., "Morphological Image Analysis-Principles and Applications", Springer-Verlag, 1999.

[4] Lin, I-I, Khoo, V., "Computer based algorithm for ship detection from ERS SAR imagery", 3rd ERS Symposium - Space at the service of our Environment,14-21 March 1997.

[5] Grasso, R., Spina, F., "Small bottom object density analysis from side scan sonar data by a mathematical morphology detector", IEEE Information Fusion, 2006 9th International Conference on, Florence, 10-13 July 2006.

[6] Crisp D. J., "The State-of-the-Art in Ship Detection in Synthetic Aperture Radar Imagery", DSTO Information Sciences Laboratory, DSTO–RR–0272